ACCSCIENCE PUBLISHING

Global Translational Medicine

ORIGINAL RESEARCH ARTICLE

Comparative evaluation of the therapeutic effects of *Schisandra chinensis* and *Schisandra sphenanthera* on vascular cognitive impairment and their drug-like compounds

Yucen Zou[1†], Bin Li[1†], Meiqi Wang[1], Xiaomeng Xie[2], Jianuo Zhang[1], Qi Xiao[1], Chunyan Yang[1], Jiushi Liu[1], Haitao Sun[1], Bengang Zhang[1], Pei Ma[1*], and Haitao Liu[1*]

[1]State Key Laboratory of Bioactive Substance and Function of Natural Medicines, Institute of Medicinal Plant Development, Chinese Academy of Medical Sciences, Peking Union Medical College, Beijing, China

Abstract

The fruits of *Schisandra chinensis* (SCF) and *Schisandra sphenanthera* (SSF) are traditional Chinese herbal medicines classified as medicinal and food homologous materials, known for their significant neuroprotective efficacy. However, the differences in their therapeutic effects and active components for the treatment of vascular cognitive impairment (VCI) remain unclear. This study aimed to elucidate the neuroprotective activities of SCF and SSF on VCI and investigate the compositional disparities between the two. The lipopolysaccharide-induced and oxygen-glucose deprivation/reoxygenation (OGD/R)-induced BV2 cell models were used to evaluate the protective effects of SCF and SSF against neuroinflammation and mitochondrial damage, respectively. The therapeutic effects were further validated using a bilateral common carotid artery stenosis mouse model. Compositional differences were analyzed using ultraperformance liquid chromatography-quadrupole time-of-flight mass spectrometry (UPLC-Q-TOF/MS), and drug-like properties of their constituents were assessed. *In vitro* experiments showed that SCF and SSF at concentrations of 6.4, 16, and 40 μg/mL reduced nitric oxide, tumor necrosis factor-alpha, and interleukin-6 levels in a dose-dependent manner. Notably, at the same concentrations, SCF significantly mitigated OGD/R-induced mitochondrial damage, whereas SSF showed no significant effect. Compared with SSF, SCF exhibited stronger anti-neuroinflammatory and antioxidant properties. *In vivo* experiments further demonstrated that SCF, administered at 400 mg/kg, was more effective in improving learning ability, spatial learning and memory, cerebral blood flow, and nerve fiber repair than SSF. Moreover, 71 and 64 compounds were identified in SCF and SSF, respectively, using UPLC-Q-TOF/MS. Drug-like property analysis of these compounds revealed that the superior therapeutic effects of SCF may be attributed to differences in biphenylcyclooctene-type lignans. Our data support the conclusion that SCF possesses significantly superior neuroprotective activity compared to SSF, providing a theoretical basis for its clinical application in VCI.

Keywords: *Schisandra chinensis*; *Schisandra sphenanthera*; Vascular cognitive impairment; Neuroinflammation; Mitochondrial damage; UPLC-Q-TOF/MS

[†]These authors contributed equally to this work.

***Corresponding authors:**
Haitao Liu
(htliu@implad.ac.cn)
Pei Ma
(pma@implad.ac.cn)

Citation: Zou Y, Li B, Wang M, *et al*. Comparative evaluation of the therapeutic effects of *Schisandra chinensis* and *Schisandra sphenanthera* on vascular cognitive impairment and their drug-like compounds. *Global Transl Med*. 2025:4(1):90-103.
doi: 10.36922/gtm.6879

Received: December 3, 2024

Accepted: December 19, 2024

Published online: February 14, 2025

Copyright: © 2025 Author(s). This is an Open-Access article distributed under the terms of the Creative Commons Attribution License, permitting distribution, and reproduction in any medium, provided the original work is properly cited.

Publisher's Note: AccScience Publishing remains neutral with regard to jurisdictional claims in published maps and institutional affiliations.

[2]The National Clinical Research Center for Mental Disorders and Beijing Key Laboratory of Mental Disorders, Beijing Anding Hospital and Advanced Innovation Center for Human Brain Protection, Capital Medical University, Beijing, China

1. Introduction

Vascular cognitive impairment (VCI) refers to a clinical syndrome characterized by the impairment of at least one cognitive function domain, caused by cerebrovascular disease and its associated risk factors.[1] It encompasses a broad spectrum of cognitive disorders, ranging from mild cognitive impairment to dementia.[2] The prevalence of VCI increases rapidly with age, making it the second most prevalent type of cognitive deficit after Alzheimer's disease.[3] The primary symptoms of VCI, including attention deficits, memory loss, language impairment, executive dysfunction, and spatial cognitive decline, significantly impact patients' quality of life.[4] Although studies have shown that medications, such as donepezil can benefit VCI patients, their clinical efficacy remains contentious.[5] This underscores the imperative for developing safe and effective therapeutic agents for VCI.

Traditional Chinese medicine (TCM) has attracted growing attention owing to its efficacy in the prevention and treatment of VCI.[6] More importantly, TCM is recognized for its safety and effectiveness, especially in managing chronic conditions.[7] Wuweizi, a well-known TCM, has been used as a tonic and sedative agent for thousands of years.[8] Modern pharmacological studies have suggested that Wuweizi possesses a range of biological activities, such as neuroprotective, anti-inflammatory, antioxidative, and hepatoprotective properties.[9-12] Historically, Wuweizi is referred to as the ripe fruit of both *Schisandra chinensis* (SCF) and *Schisandra sphenanthera* (SSF). However, since the 2000 edition of Chinese Pharmacopoeia (ChP), SCF and SSF have been classified as distinct crude drugs with independent quality standards, despite similarities in their described efficacies in ChP.[13]

Dibenzocyclooctadiene lignans are the major bioactive components responsible for many of the pharmacological activities of SCF and SSF.[14,15] Compounds, such as schisandrol A-B, schisandrin A-C, and schisantherin A are present in both SCF and SSF, although their quantities differ, potentially contributing to both similar and distinct pharmacological effects.[13] Recent studies have highlighted the neuroprotective properties of SCF and its major constituents, particularly dibenzocyclooctadiene-type lignans, including schisandrin A, schisandrin B, schisandrin C, schisantherin A, schisandrin, schisandrol B, gomisin A, and gomisin N. These compounds have demonstrated protective effects against neurodegenerative and hypoxia-ischemia-related neural injuries, including stroke, Alzheimer's disease, and Parkinson's disease.[16-20] In contrast, research on SSF remains relatively limited. It is unclear whether SCF and SSF exhibit significant therapeutic effects against VCI. The differences in pharmacological efficacy and contributing constituents between SCF and SSF are also uncertain.

In this study, we evaluated the therapeutic differences between SCF and SSF in VCI using *in vivo* and *in vitro* models, characterized their chemical composition through ultraperformance liquid chromatography-quadrupole time-of-flight mass spectrometry (UPLC-Q-TOF/MS), and evaluated the drug-like properties of their components. The findings aim to provide valuable insights into the pharmacological difference of SCF and SSF against VCI and offer a reference for their clinical applications.

2. Materials and methods

2.1. Cell culture

BV2 cells were cultured in Dulbecco's Modified Eagle Medium (DMEM) supplemented with 10% fetal bovine serum (Gibco, USA). Cells at 80% – 90% confluence were used for experiments. For neuroinflammation modeling, BV2 cells were seeded into 96-well plates at a density of 3×10^5 cells/mL, pretreated with SCF or SSF (at concentrations of 0 – 40 μg/mL) for 2 h, and subsequently stimulated with lipopolysaccharide (LPS, 1 μg/mL, Sigma, Germany) for 24 h. For the oxygen and glucose deprivation/reperfusion (OGD/R) model, SCF- or SSF-pretreated cells were incubated in oxygen deprivation (94% N_2 + 5% CO_2 + 1% O_2) and glucose-free DMEM for 6 h, followed by normal incubation for an additional 6 h.

2.2. Cell viability assay

Cells were assessed using the Cell Counting Kit-8 (CCK8, Solarbio, China) according to the manufacturer's protocol. Cells were incubated with CCK8 solution (10% v/v) for 1.5 h. Absorbance was measured at 450 nm using a microplate reader (Spark, Tecan, Switzerland).

2.3. Griess and ELISA assay for inflammatory cytokines

After treatment, cell culture supernatants were collected and centrifuged. The levels of nitric oxide (NO) in cell supernatants were determined using commercial kits (Griess, Beyotime Biotechnology, China) according to the manufacturer's instructions, and absorbance was measured at 540 nm using a microplate reader (Spark,

Tecan, Switzerland). While, the concentrations of tumor necrosis factor-alpha (TNF-α) and interleukin-6 (IL-6) were measured using ELISA kits (Cat. no: 431304 [IL-6], Cat. no: 430915 [TNF-α], Biolegend, USA) according to the manufacturer' s protocol.

2.4. Measurement of mitochondrial membrane potential

The mitochondrial membrane potential was assessed using a JC-1 kit (Beyotime, China) under OGD/R conditions. Cells were incubated with JC-1 working buffer in the dark for 30 min, following the manufacturer's protocol. Fluorescence signals representing mitochondrial membrane potential levels were detected using a fluorescence microscope at excitation/emission wavelengths of 514/529 nm (for JC-1 monomers) and 585/590 nm (for JC-1 aggregates).

2.5. Animal models and treatment protocols

All animal experiments were approved by the Committee on Use and Care of Animals of the Institute of Medicinal Plant Development. A total of 50 10-week-old male C57BL/6J mice (weighing 24 – 29 g) were provided by Vital River Laboratory Animal Technology (China) and acclimated to laboratory conditions for 7 days. The mice were randomly divided into five groups (n = 10 per group):

(i) Control (CON): Sham operation with no treatment.
(ii) Model (MOD): Bilateral common carotid artery stenosis (BCAS) surgery with vehicle treatment (0.5% sodium carboxymethyl cellulose [CMC-Na]).
(iii) Positive control (POS): BCAS surgery with 20 mg/kg of nimodipine (Bayer, Germany)
(iv) SCF group: BCAS surgery with 400 mg/kg SCF extract.
(v) SSF group: BCAS surgery with 400 mg/kg of SSF extract.

Mice were anesthetized, and both common carotid arteries (CCAs) were exposed. BCAS was induced using microcoils (0.18 mm inner diameter; Sawane Spring Co, Japan) following established protocols.[21] The microcoil was first applied to the right CCA by rotating it around the artery and then to the left CCA after a 30-min interval. Sham-operated control mice underwent the same surgical procedure without the placement of microcoils. Seven days post-surgery, BCAS mice in different groups received daily intragastric administration of the corresponding drug treatments for 30 consecutive days, while the CON and MOD groups received 0.5% CMC-Na as vehicle controls.

2.6. Neurological severity score test

Neurological function was evaluated using the modified neurological severity score (mNSS) test[22] on days 7, 14, 21, and 28 post-BCAS. The mNSS is a composite assessment of motor function (muscle status, abnormal movements), sensory function (visual, tactile, and proprioceptive), and reflexes. Scores range from 0 (normal) to 18 (maximal deficit), with higher scores indicating greater neurological impairment.

2.7. Open field test

Behavioral activity was assessed on day 29 using the open field test. Mice were placed individually in the center of a 50 × 50 × 50 cm white box, and their total distance traveled (in mm) was recorded over 5 min using a video analysis system (v5.2.0.0, SuperMaze, China).

2.8. Novel object recognition test (NORT)

Cognitive abilities were evaluated using the NORT from days 30 to 33. During the first 3 days, mice acclimated daily to a 50 × 50 × 50 cm white box containing two identical red cylinders placed at opposite ends. Tests were conducted on the 4th day in two phases:

(i) Phase 1: Mice were allowed to explore two identical cylinders (F1 and F2) for 5 min. The exploration time for each object was recorded, and the relative preference index was calculated as

$$RPI(\%) = \frac{F1 - F2}{F1 + F2} \times 100 \quad \text{(I)}$$

(ii) Phase 2: After a 30-min rest period, one cylinder was replaced with a new green square of the same height. Mice were allowed to explore the new object (N) and the remaining cylinder (F) for 5 min. The exploration time was recorded, and the relative discrimination index was calculated as follows:

$$RDI(\%) = \frac{N - F}{N + F} \times 100 \quad \text{(II)}$$

Exploration behaviors were recorded and analyzed using SuperMaze software.

2.9. Morris water maze (MWM) test

Spatial learning deficits were assessed twice daily using an enhanced MWM test from days 33 to 37. A 1-m-diameter pool was placed in a room devoid of external orientation cues and divided into four quadrants with four fixed points using the SuperMaze system. An invisible, submerged platform was fixed in the northwest quadrant. Mice were randomly placed at one of the designated starting points and were allowed 1.5 min to locate the platform, with a 10-s stay permitted upon successful navigation. Mice unable to find the platform were passively placed on it for 10 s. On day 38, the platform was removed, and mice underwent a free swim test for 1.5 min to evaluate spatial reference memory. The time taken to reach the previous

platform location and other behavioral data were analyzed using SuperMaze software.

2.10. Full-field laser perfusion imaging

One hour after final administration, anesthetized mice were subjected to craniotomy for full-field laser perfusion imaging (FLPI) (FLPI2, Moor Instruments, United Kingdom). The FLPI system was configured to a low-resolution, high-speed imaging mode with a display rate of 25 Hz, a time constant of 1.0 s, and an exposure time of 20 ms. Every measurement lasted 1 min, generating six stabilized blood flow images with the camera positioned 10 cm above the brain.

2.11. Luxol fast blue (LFB) staining

On day 40, anesthetized mice received transcardial perfusion with saline followed by paraformaldehyde. Brains were post-fixed, embedded in paraffin, sectioned into 4-μm slices, and stained with 0.1% LFB, followed by 0.05% lithium carbonate. The sections were then sealed with a coverslip and examined under a light microscope. The severity of demyelination was scored as follows: 0: normal; 1: disarrangement of nerve fibers; 2: obvious vacuoles; and 3: injured and disappearance of myelinated fibers.

2.12. Immunohistochemistry staining

Paraffin sections underwent antigen retrieval, treatment with 3% H_2O_2, and blocking with 3% bovine serum albumin. Sections were incubated overnight at 4°C with a rabbit anti-myelin basic protein (MBP) antibody (1:1000; Cat. no. K002910P, Solarbio, China), followed by incubation with horseradish peroxidase-labeled anti-rabbit secondary antibody (1:200; Cat. no. PV-9000, Solarbio, China) and diaminobenzidine staining. The sections were counterstained with hematoxylin and examined under a light microscope. The degree of demyelination was semi-quantified using Image-Pro Plus software.

2.13. Ethanol extract preparation for SCF and SSF

SCF and SSF fruits were harvested from Huanren (Jilin province) and Shangluo (Shaanxi province), China, respectively, in September 2020. The samples were identified by Dr. Yaodong Qi (Institute of Medicinal Plant Development, Chinese Academy of Medical Sciences), and voucher specimens were stored in the authors' laboratory. The dried fruit (500 g) was powdered, extracted using gradient ethanol (1:10 v/v), and enriched to obtain an ethanol extract.

2.14. Chemical constituent analysis of SCF and SSF

SCF and SSF extracts were analyzed using ACQUITY UPLC coupled with a Xevo G2 QTOF detector (Waters Corporation, United States). Major constituents were separated using an ACQUITY UPLC BEH C_{18} column (2.1 × 100 mm, 1.7 μm) at a flow rate of 0.3 mL/min and a temperature of 23°C, with an injection volume of 2 μL. The elution gradient was performed using 0.1% formic acid water (A) and acetonitrile (B) as follows: 0 – 1 min, 5% – 30% B; 1 – 2 min, 30% – 40% B; 2 – 4 min, 40% – 52% B; 4 – 6 min, 52% – 60% B; 6 – 9 min, 60% – 62% B; 9 – 10 min, 62% B; 10 – 13 min, 62% – 66% B; 13 – 15 min, 66% – 70%. Mass weight was detected in centroid mode using an electrospray ionization source over a mass range of 50 – 1700 Da, with a scan time of 0.3 s. The MS detector was set with a capillary voltage of 3 kV, a sampling cone voltage of 40 V, a source temperature of 100°C, a desolvation temperature of 350°C, and collision energy of 6 kV. Data were collected using MassLynx 4.1 software and profiled using Progenesis QI 2.3 software, with assistance from a self-constructed *Schisandra* compound database.

2.15. Evaluation of drug-likeness

For compounds identified using UPLC-Q-TOF/MS, six physicochemical properties, including lipophilicity, size, polarity, solubility, saturation, and flexibility, were evaluated for bioavailability. Predictions of passive human gastrointestinal absorption (HIA), blood-brain barrier (BBB) permeability, and interactions with permeability glycoprotein (P-gp) for active efflux were conducted using the SwissADME web tool (http://www.swissadme.ch).

2.16. Statistical analysis

Raw data were presented as mean ± SEM. One-way ANOVA was used for multiple group comparisons in GraphPad Prism 8.0, followed by Fisher's least significant difference test for normally distributed data, or the Kruskal–Wallis *H*-test for non-normally distributed data. Statistical significance was set at $P < 0.05$ or $P < 0.01$.

3. Results

3.1. SCF exhibits stronger anti-neuroinflammatory activity than SSF in LPS-induced BV2 cells model

Microglial activation is a prominent feature following chronic cerebral hypoperfusion.[23] To evaluate and compare the anti-neuroinflammation effects of SCF and SSF, an LPS-induced BV2 cell model was established. A pilot study (data not shown) confirmed that SCF and SSF had no significant effects on BV2 cell viability at concentrations below 80 μg/mL. Based on preliminary experimental results, 40, 16, 6.4, and 2.56 μg/mL were selected for further study.

As shown in Figure 1, LPS stimulation significantly increased the production of NO, TNF-α, and IL-6 in BV2 cells compared to the control group. Treatment with

SCF or SSF (40 and 16 μg/mL) significantly reduced NO and TNF-α levels. Furthermore, IL-6 production was markedly suppressed in BV2 cells treated with SCF or SSF at the highest dose (40 μg/mL). Notably, the reduction in inflammatory markers was more pronounced in the SCF group than in the SSF group at the same dose.

3.2. SCF ameliorates OGD/R-induced mitochondrial damage in BV2 cells

Mitochondrial damage serves as an indicator of oxidative stress and is relevant to studies on antioxidant-induced mitochondrial damage models.[24] To examine the effects of SCF and SSF on mitochondrial integrity, an OGD/R-BV2 cells model was employed. As shown in Figure 2, OGD/R treatment significantly decreased both cell viability and mitochondrial membrane potential in BV2 cells. Treatment with SCF (40, 16, and 6.4 μg/mL) resulted in a dose-dependent restoration of these parameters, whereas SSF had no significant effect. These results suggest that SCF provides superior mitochondrial protection compared to SSF.

3.3. SCF is more efficacious than SSF in alleviating cognitive impairment in BCAS mice

The BCAS mouse model is widely used to study aspects of VCT. To determine whether SCF or SSF treatment alleviates

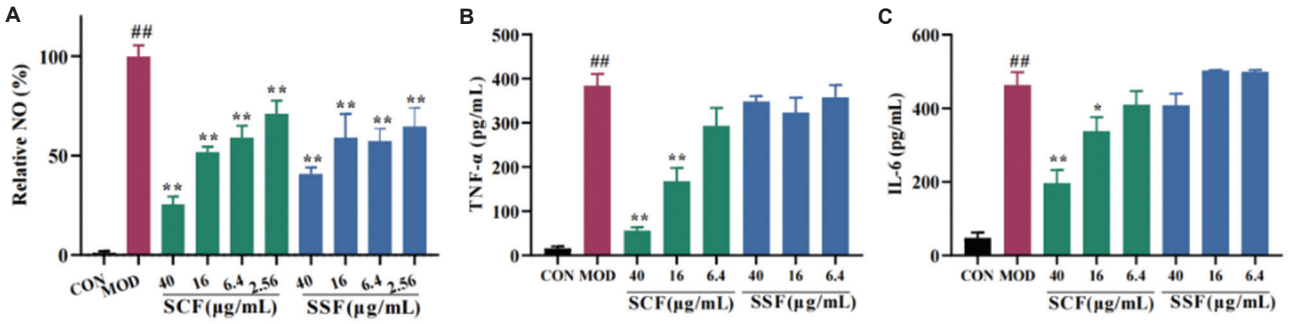

Figure 1. Comparative effects of SCF and SSF on neuroinflammation in LPS-induced BV2 cells. The production of (A) NO, (B) TNF-α, and (C) IL-6 was inhibited following SCF or SSF treatment. Data are presented as mean ± SEM (n = 3 per group). Notes: $^{*}P < 0.05$ and $^{**}P < 0.01$, compared with LPS-treated models (MOD); $^{\#}P < 0.05$ and $^{\#\#}P < 0.01$, compared with the control (CON).
Abbreviations: SCF: *Schisandra chinensis;* SSF: *Schisandra sphenanthera;* LPS: Lipopolysaccharide; NO: Nitric oxide; TNF-α: Tumor necrosis factor-alpha; IL-6: Interleukin-6.

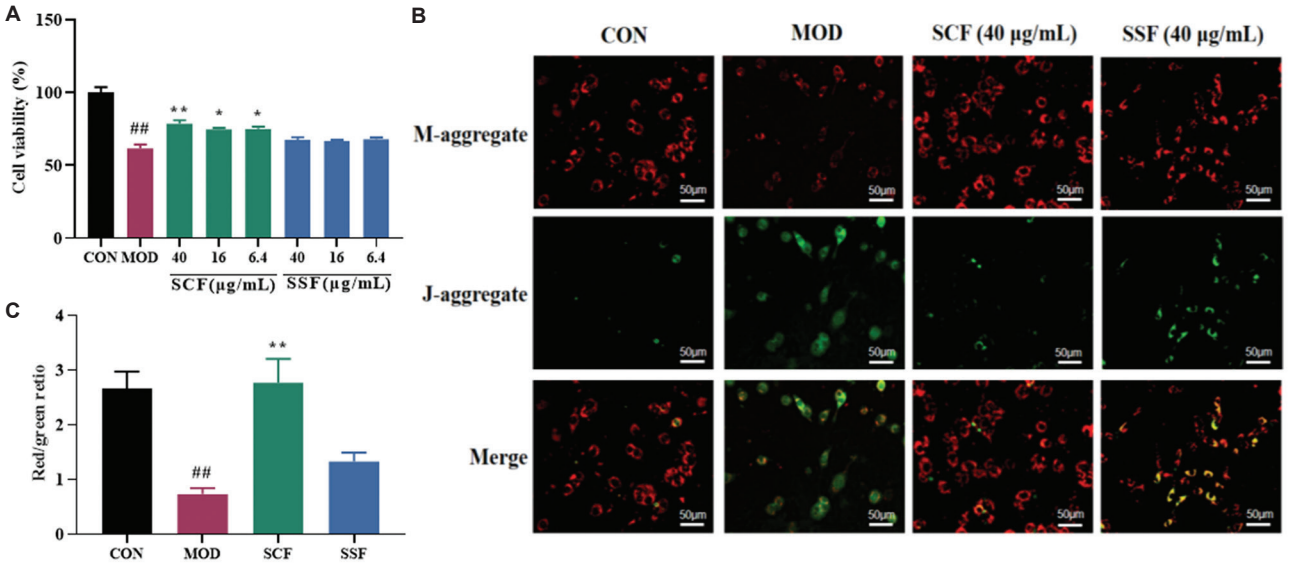

Figure 2. Comparative effects of SCF and SSF on cell viability and mitochondrial membrane potential in OGD/R-induced BV2 cells. (A) Cell viability. (B) Representative photomicrographs of JC-1 staining (Scale bars: 50 μm; magnification: 200×) and (C) corresponding quantification analysis. Data are presented as mean ± SEM (n = 3 per group). Notes: $^{*}P < 0.05$ and $^{**}P < 0.01$, compared with OGD/R-treated model (MOD); $^{\#}P < 0.05$ and $^{\#\#}P < 0.01$, compared with control (CON).
Abbreviations: SCF: *Schisandra chinensis;* SSF: *Schisandra sphenanthera.*

cognitive impairment, several behavioral experiments were conducted in BCAS mice. The mNSS revealed no significant limb-curl and tail-lift reflexes among all groups at 7, 14, 21, and 28 days post-operatively (Figure 3A), indicating normal neurological function and ensuring that cognitive impairment assessments were not confounded by motor deficits. Similarly, the open field test showed no significant differences in total distances traveled (Figure 3B), implying that BCAS surgery did not affect motor or optic nerve function.

Furthermore, during the NORT, no significant preference differences were observed for two old objects among groups during the training phase (Figure 3C). However, after BCAS surgery, mice exhibited reduced curiosity toward the new object, as indicated by a significantly decreased relative discrimination index in the MOD group compared to the CON group ($P < 0.05$) (Figure 3D). Notably, SCF (400 mg/kg) treatment significantly restored exploratory preference compared to the MOD group ($P < 0.05$), whereas SSF (400 mg/kg) showed a trend toward cognitive improvement without statistical significance ($P > 0.05$).

In the MWM test, baseline escape latency showed no significant difference among groups. However, BCAS mice exhibited a significant increase in escape latency on days 3 – 5 ($P < 0.01$, compared to control mice). SCF treatment significantly reduced the escape latency ($p<0.01$) (Figure 3E). During the spatial exploration test, BCAS mice in the MOD group exhibited a significantly decreased number of platform crossing ($P < 0.01$) (Figure 3F), a significantly decreased frequency of target quadrant crossing ($P < 0.01$) (Figure 3H), and less time spent in

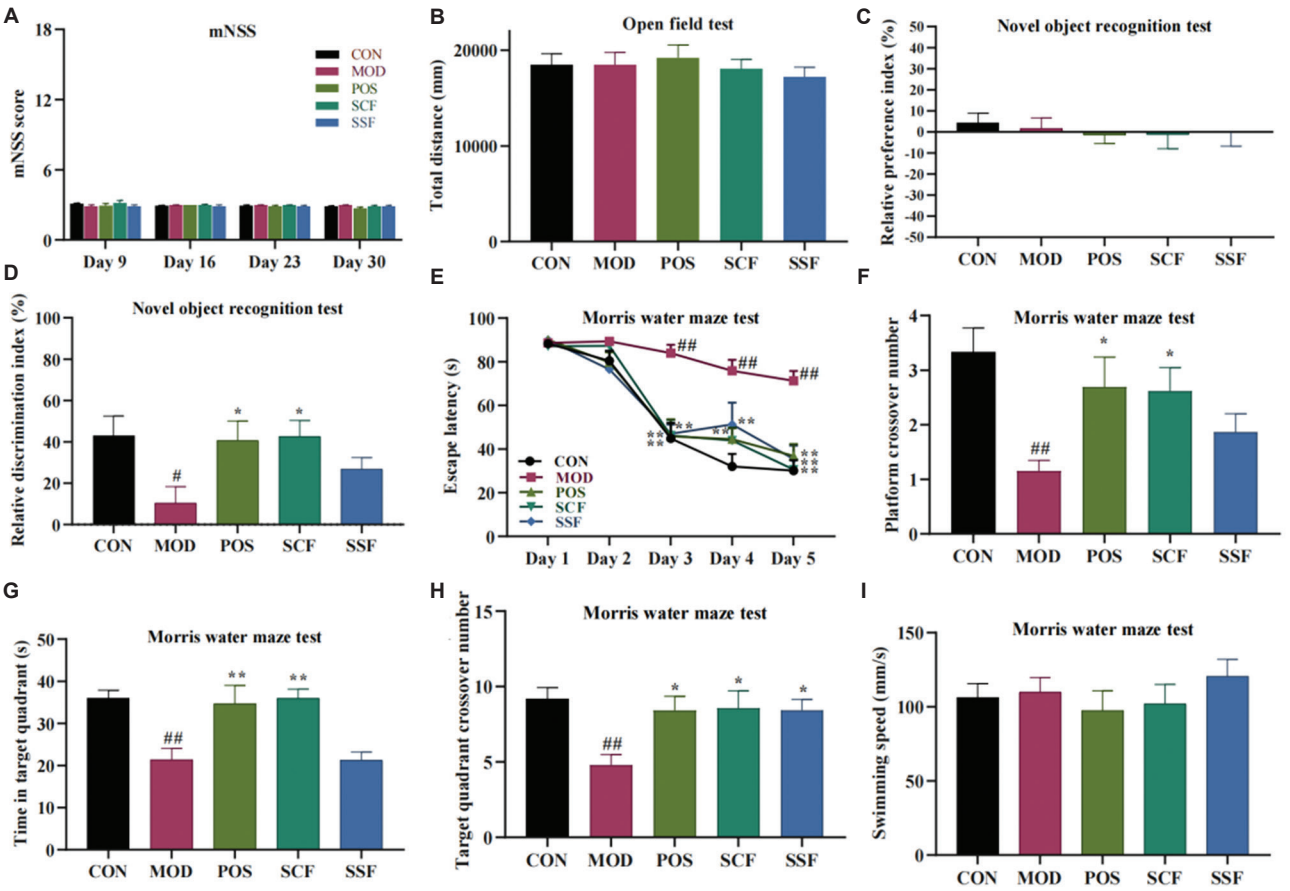

Figure 3. Effects of SCF and SSF on exploratory locomotor behavior and spatial learning memory following BCAS surgery. (A) mNSS at different time points. (B) Total distance traveled in the open field test on day 29 post-BCAS. (C) Relative preference index and (D) relative discrimination index in the novel object recognition test on day 32. (E) Escape latency in Morris water maze navigation test at different time points. (F-I) Frequency of platform crossings, time spent in the target quadrant, frequency of target quadrant crossings, and swimming speed in the Morris water maze probe test on day 38. Data are presented as mean ± SEM ($n = 8$ per group). Notes: $^{*}P < 0.05$ and $^{**}P < 0.01$, compared with the BCAS group (MOD); $^{\#}P < 0.05$ and $^{\#\#}P < 0.01$, compared with the control group (CON). POS: Positive control.
Abbreviations: SCF: *Schisandra chinensis;* SSF: *Schisandra sphenanthera;* BCAS: Bilateral common carotid artery stenosis; mNSS: Modified neurological severity score.

the target quadrant ($P < 0.01$) (Figure 3G). In contrast, SCF-treated mice demonstrated better spatial learning and memory ability than the MOD mice, as evidenced by a significantly increased frequency of platform crossing ($P < 0.05$), a higher frequency of target quadrant crossings ($P < 0.05$), and significantly more time spent in the target quadrant ($P < 0.01$). However, the cognitive improvement effects of SSF were less pronounced and not statistically significant ($P > 0.05$). In addition, no significant differences in swimming speed were observed among groups ($P > 0.05$) (Figure 3I). Overall, these behavioral assessments demonstrate that SCF treatment significantly ameliorates learning and memory deficits in BCAS mice.

3.4. SCF and SSF improves cerebral blood flow

As shown in Figure 4, cerebral blood flow was significantly reduced due to hypoperfusion induced by BCAS surgery ($P < 0.01$). In comparison to untreated BCAS mice, all drug-treated groups exhibited increased cerebral blood flow ($P < 0.01$), indicating that both SCF and SSF improved cerebral perfusion following BCAS surgery.

3.5. SCF is more efficacious than SSF in alleviating BCAS-induced white matter injury

In CON mice, LFB staining revealed a densely packed and well-organized myelin sheath. In contrast, MOD mice exhibited a disrupted myelin structure, characterized by a loose and disordered myelin sheath and the presence of white vacuoles in the corpus callosum (Cc, paramedian), fimbria of the hippocampus (Fi), ventral posteromedial thalamic nucleus (VPT), and caudate putamen (Cpu, striatum) ($P < 0.01$) (Figure 5). All drug-treated mice exhibited significantly preserved white matter integrity ($P < 0.05$ or $P < 0.01$). Notably, the SCF group showed a greater degree of preservation, with denser and more organized nerve fibers than the SSF group.

The MBP immunohistochemical staining results (Figure 6) were consistent with the LFB staining data. Compared with CON mice, the MOD mice exhibited significantly reduced and weaker MBP staining in the Cc, Fi, VPT, and Cpu ($P < 0.01$ or $P < 0.05$). SCF treatment significantly alleviated myelin degeneration in all four brain areas ($P < 0.01$ or $P < 0.05$), whereas SSF treatment exerted significant protective effects only in VPT and Cpu ($P < 0.01$)

3.6. Chemical characterization of SCF and SSF using UPLC-Q-TOF/MS

The chemical compositions of SCF and SSF were analyzed using UPLC-Q-TOF/MS (Figure 7). A total of 71 compounds were identified in SCF, including 56 lignans (42 diphenylcyclooctene lignans, 8 tetrahydrofuran

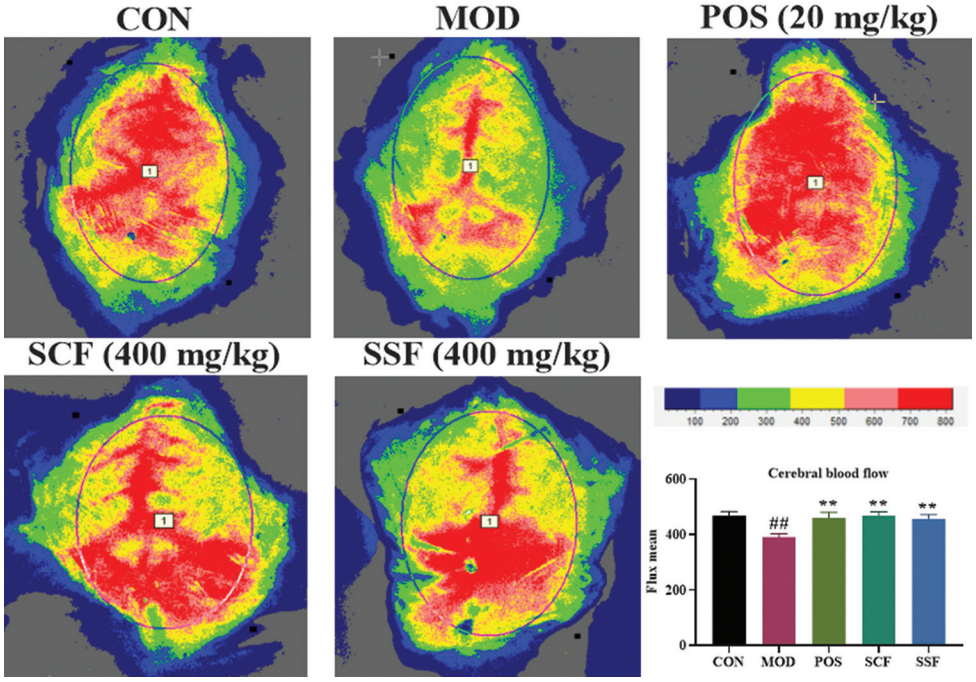

Figure 4. Representative images and related quantitative analysis for comparative effects of SCF and SSF on cerebral blood flow following BCAS surgery. The color bar (blue to red) indicates low to high flow velocity. Data are presented as mean ± SEM ($n = 8$ per group). Notes: $^{*}P < 0.05$ and $^{**}P < 0.01$, compared with the BCAS group (MOD); $^{\#}P < 0.05$ and $^{\#\#}P < 0.01$, compared with the control group (CON).
Abbreviations: POS: Positive control; SCF: *Schisandra chinensis;* SSF: *Schisandra sphenanthera;* BCAS: Bilateral common carotid artery stenosis.

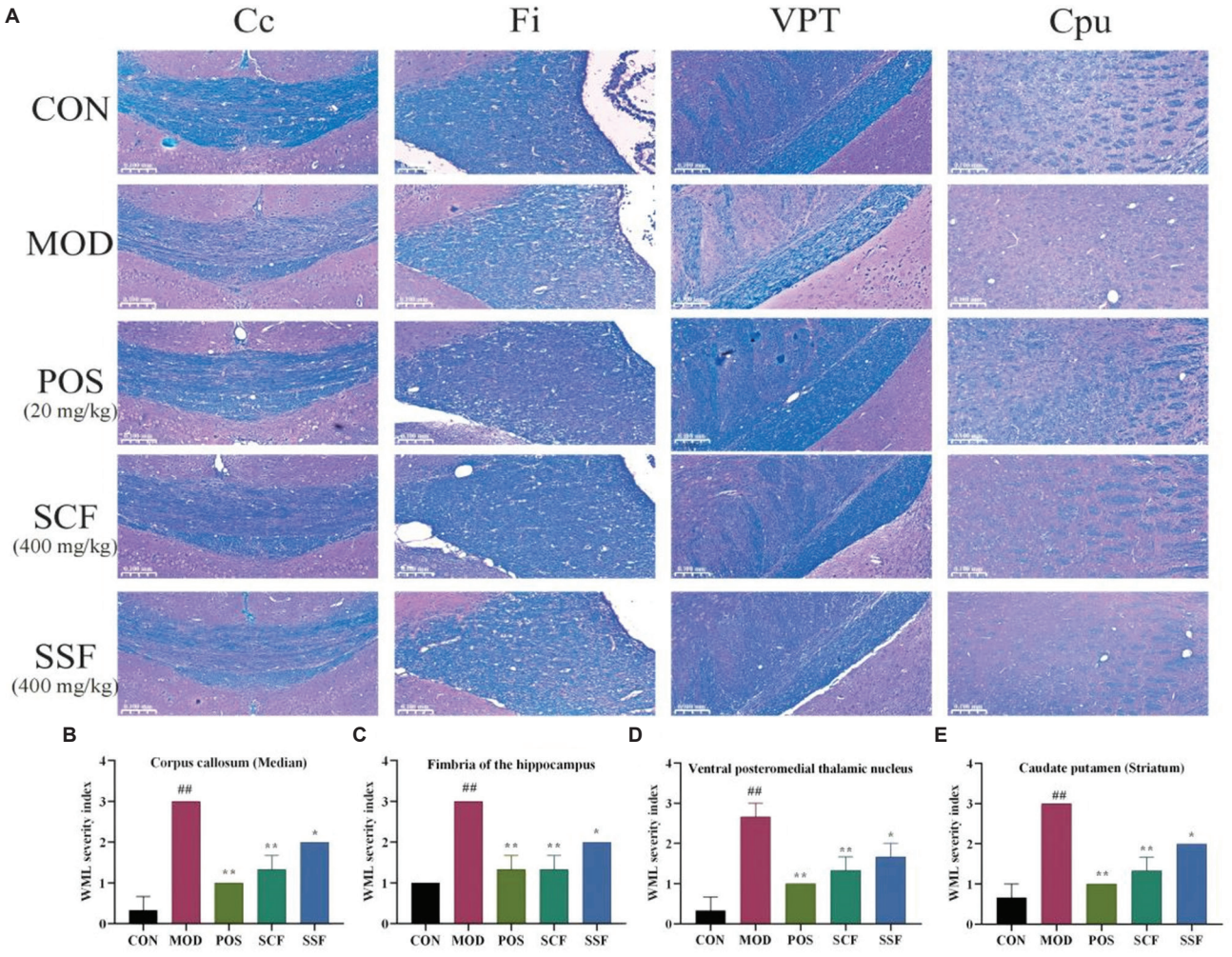

Figure 5. Comparative effects of SCF and SSF on white matter integrity following BCAS surgery. (A) LFB-stained images showing increased myelin rarefaction and white matter lesion formation in the Cc (paramedian), fimbria of the hippocampus (Fi), ventral posteromedial thalamic nucleus (VPT), and Cpu (striatum) of BCAS mice, with a visible protective effect in the SCF- and SSF- treated groups. All images were taken under identical exposures and conditions (Scale bar: 200 μm; magnification: 20×). (B-E) Quantification analysis of LFB-staining in Cc, Fi, VPT, and Cpu, respectively. Data are presented as mean ± SEM (n = 3 per group). Notes: $^{*}P < 0.05$ and $^{**}P < 0.01$, compared with the BCAS group (MOD); $^{\#}P < 0.05$ and $^{\#\#}P < 0.01$, compared with the control group (CON).
Abbreviations: POS: Positive control; SCF: *Schisandra chinensis;* SSF: *Schisandra sphenanthera;* BCAS: Bilateral common carotid artery stenosis; Cc: Corpus callosum; Cpu: Caudate putamen.

lignans, 4 furofurans, 2 lignan lactones), 10 carboxylic acids (5 eicosanoids, 5 carboxylic acids), 2 lactones, 2 sesterterpenoids, and 1 pyrrilium (Table S1). For SSF, a total of 63 compounds were identified, including 21 lignans (9 diphenylcyclooctene lignans, 4 dibenzylbutane lignans, 5 tetrahydrofuran lignans, 2 aryltetralin lignans, 1 furanoid lignan), 2 terpenoids (1 triterpenoid, 1 sesquiterpenoid), 1 lactone, 17 phenylpropanoids (16 phenylpropanoids, 1 flavonoid), 1 phenol, 16 alkaloids, 4 carboxylic acids, and 1 sulfoxide (Table S2). These results suggest that SCF and SSF exhibit distinct chemical compositions, which may contribute to different pharmacological effects.

3.7. Pharmacokinetic differences between compounds in SCF and SSF

Compounds with high bioavailability and drug-likeness properties are more likely to be absorbed.[25] Bioactive compounds with therapeutic effects are generally expected to exhibit passive HIA properties.[26] Therefore, we further conducted analysis of six physicochemical properties, HIA and BBB permeation, and interactions with P-gp in the identified compounds.

As shown in Figure 8, the predicted lipophilicity, size, polarity, solubility, flexibility, and saturation properties were evaluated for the identified compounds. A total of 64 compounds in SCF and 60 compounds in SSF were

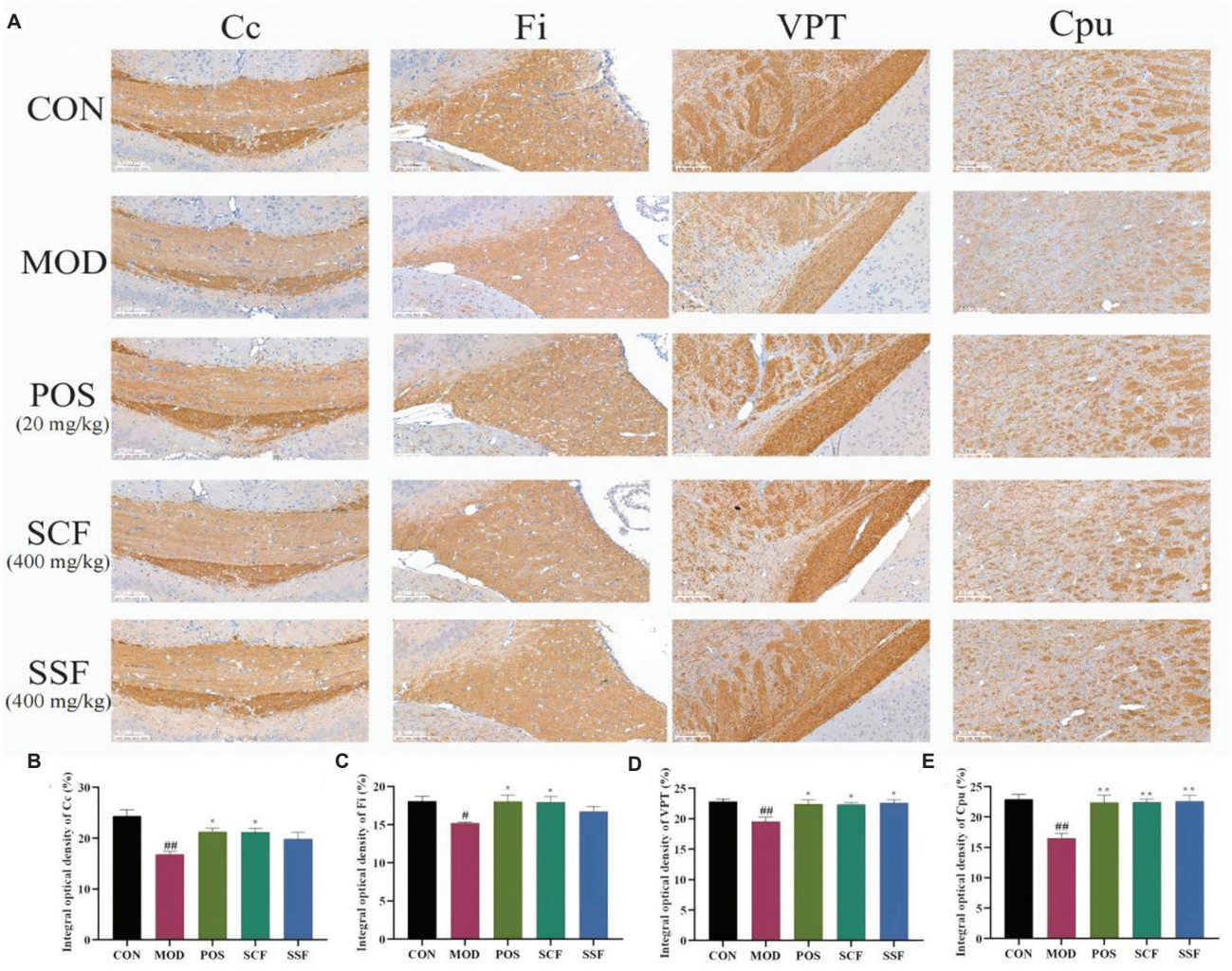

Figure 6. Comparative effects of SCF and SSF on myelin regeneration following BCAS surgery. (A) MBP immunoreactivity was reduced in the Cc, fimbria of the hippocampus (Fi), ventral posteromedial thalamic nucleus (VPT), and Cpu of BCAS mice. A trend of alleviation was observed in the positive control (POS), SCF-, and SSF-treated groups. All images were taken under identical exposures and conditions (Scale bar: 200 μm; magnification: 100×). (B-E) Quantification analysis of MBP in Cc, Fi, VPT, and Cpu, respectively. Data are presented as mean ± SEM (n = 3 per group). Notes: $^{*}P < 0.05$ and $^{**}P < 0.01$, compared with the BCAS group (MOD); $^{\#}P < 0.05$ and $^{\#\#}P < 0.01$, compared with the control group (CON).
Abbreviations: POS: Positive control; SCF: *Schisandra chinensis;* SSF: *Schisandra sphenanthera;* BCAS: Bilateral common carotid artery stenosis; Cc: Corpus callosum; Cpu: Caudate putamen; MBP: Myelin basic protein.

predicted to have HIA > 25% and bioavailability > 0.15. Among these highly absorbable compounds, lignans constituted a significant portion. Furthermore, P-gp interaction analysis revealed that:

(i) In SCF, 5 carboxylic acids and 2 lignans (1 furofuran lignan, 1 diphenylcyclooctene lignan) exhibited unacceptable P-gp interaction values.
(ii) In SSF, 1 phenylpropanoid and 2 carboxylic acids showed unacceptable P-gp interaction values.
(iii) None of the compounds in SCF and only 1 compound in SSF with poor passive gastrointestinal absorption were identified as P-gp substrates, indicating low potential for active transport.

These results indicate that lignans, particularly diphenylcyclooctene-type lignans, may be key contributors to the pharmacological differences between SCF and SSF in the treatment of VCI.

4. Discussion

VCI is a cognitive dysfunction syndrome characterized by neurodegeneration, memory impairment, and cognitive deficits, for which there is currently no effective treatment.[27] Considerable evidence indicates that neuroinflammation and oxidative stress are important factors contributing to the occurrence and development of VCI.[28,29] Neuroinflammation has been

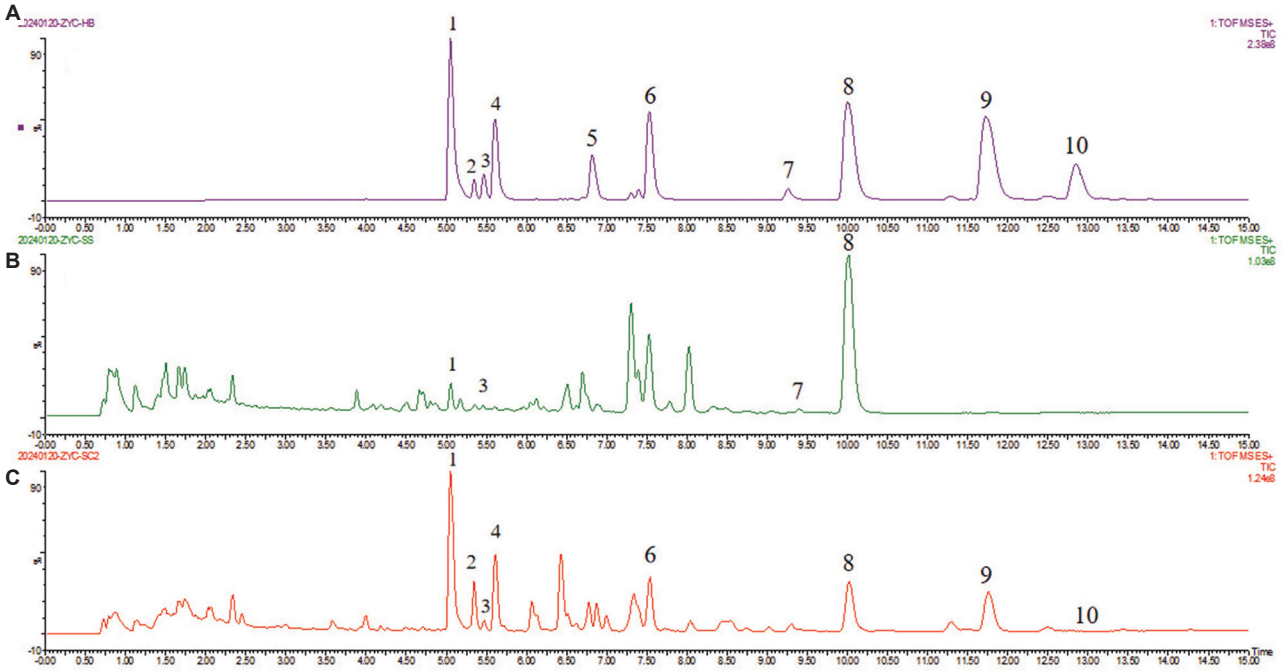

Figure 7. Total ions chromatogram of (A) standard compounds, (B) SSF, and (C) SCF in positive ion mode. Identified peaks: 1. schisandrin, 2. gomisin D, 3. gomisin J, 4. schisandrol B, 5. gomisin G, 6. schisantherin B, 7. anwulignan, 8. schisandrin A, 9. schisandrin B, 10. schisandrin C.
Abbreviations: SCF: *Schisandra chinensis;* SSF: *Schisandra sphenanthera.*

proven to contribute to the etiology of hypoxia-ischemia-induced neural injury.[30] Potential molecular mechanisms underlying VCI include inflammation and mitochondrial dysfunction.[31] Inflammatory cytokines, chemokines, and reactive oxygen and nitrogen species exacerbate neuronal damage and act as pivotal mediators of persistent neuronal injury.[32]

Previous studies have demonstrated that SCF and SSF exhibit a range of pharmacological activities, including neuroprotective, anti-inflammatory, antioxidative, and cardioprotective effects.[8,13] Notably, SCF has been shown to regulate inflammatory responses and inflammation-induced damage to cerebral vessels and brain tissue, thereby improving cerebral ischemia and neurological dysfunction.[33] Furthermore, SCF is capable of scavenging reactive oxygen species and mitigating oxidative stress-induced brain tissue damage, thereby alleviating symptoms associated with cerebral ischemia.[34]

Given the role of neuroinflammation and oxidative stress in VCI pathogenesis, we first investigated the effects of SCF and SSF in LPS- and OGD/R-induced BV2 cell models. Our data suggest that SCF exerts strong anti-neuroinflammatory and antioxidative effects in BV2 cells. Notably, SCF demonstrated significantly greater anti-neuroinflammatory and antioxidative capacity compared to SSF.

The ameliorative effects of SCF and SSF on VCI were further validated using a BCAS mouse model. This model is regarded as the most widely used experimental model for VCI,[35] as it reliably replicates both clinical and pathological features of the disease.[36] The BCAS model induces cognitive impairment, chronic hypoperfusion, and subsequent white matter damage.[21] Notably, BCAS mice do not develop cerebral infarctions and optic nerve damage but exhibit hippocampal neuronal death and atrophy, leading to learning and memory deficits.

As expected, SCF and SSF treatment significantly improved learning ability, spatial memory, and cerebral blood flow, and promoted nerve fiber repair. However, SCF was more effective than SSF in improving learning ability and spatial memory. Our results demonstrate that SCF exhibits superior efficacy in preventing white matter damage and cognitive decline, aligning with its traditional medicinal applications. However, there remains a lack of relevant research to elucidate the specific mechanisms underlying the pharmacological differences between SCF and SSF.

To address this issue, UPLC-Q-TOF/MS was used to comprehensively characterize and determine the chemical composition of SCF and SSF, as well as to evaluate the drug-like properties of their components. A total of 71 were identified in SCF, whereas 64 compounds were identified

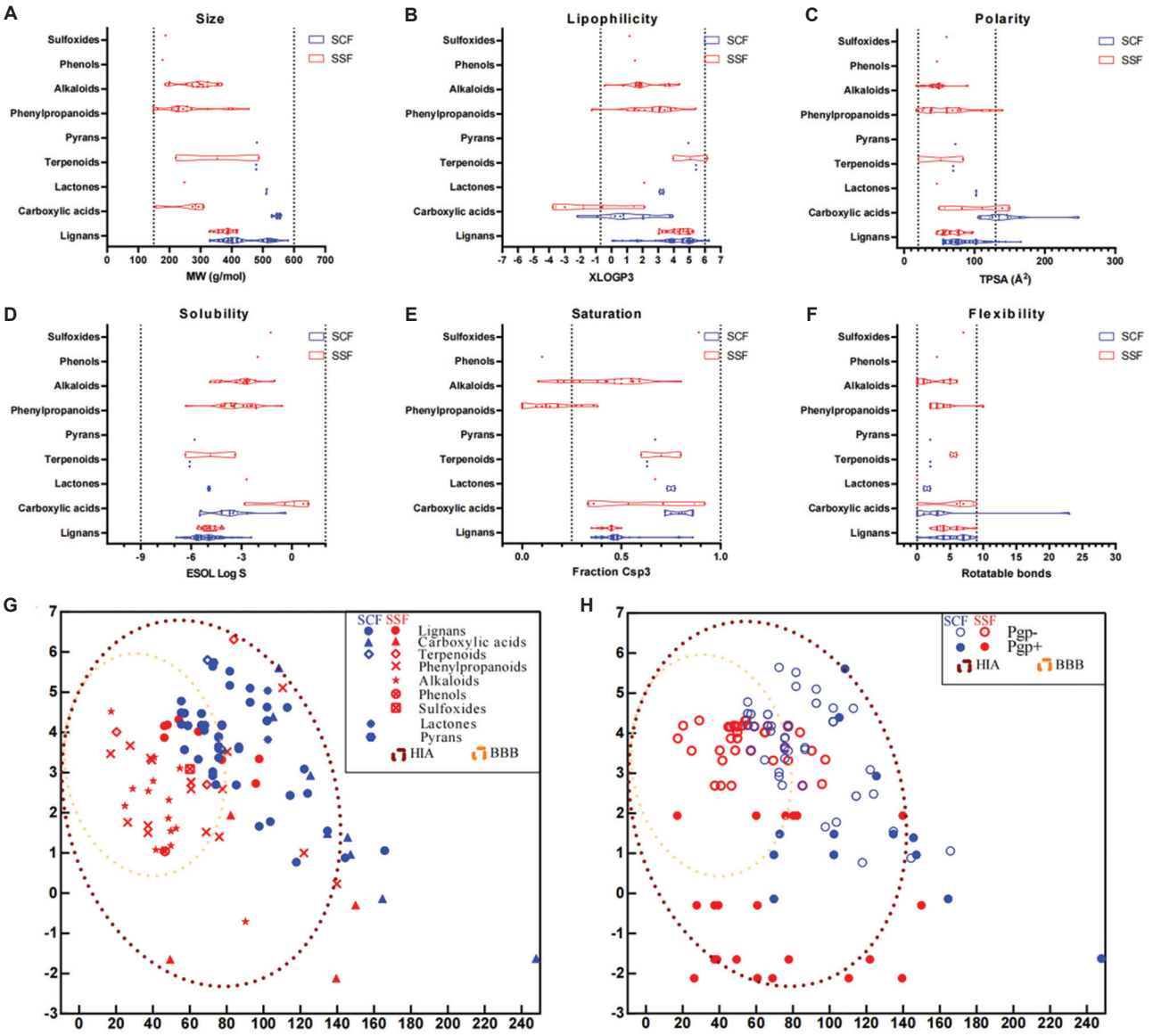

Figure 8. Drug-likeness properties and structures of identified compounds in SCF and SSF. (A-F) Six physicochemical properties for evaluating bioavailability (size, lipophilicity, polarity, solubility, saturation, and flexibility). Acceptable MW range: 150 – 600 g/moL; XLOGP3: −0.7 – 6.0; TPSA: 20 – 130 Å2; log S: −9 – 2; sp3 hybridized carbon atoms in the molecule: >0.25; number of rotatable bonds: <9. (G) Absorption, distribution, metabolism, and excretion (ADME) properties: Passive HIA and BBB permeation. (H) ADME properties: Interaction with P-gp substrates.
Abbreviations: SCF: *Schisandra chinensis;* SSF: *Schisandra sphenanthera;* MW: Molecular weight; TPSA: Topological polar surface area; HIA: Human intestinal absorption; P-gp: Permeability glycoprotein.

in SSF. SCF contained a higher number of lignans than SSF (56 vs. 16), while SSF contained more phenylpropanoids (16 vs. 0) and alkaloids (16 vs. 0).

Modern pharmacological research has demonstrated that lignans are the major bioactive constituents of SCF and SSF.[13] Particularly, dibenzocyclooctadiene lignans are regarded as the primary contributors to their pharmacological effects, which may account for their observed differences in efficacy.[13] Our data also include simulation results on compound permeability across the BBB. In SCF, the active compounds capable of effectively crossing the BBB predominantly belong to the biphenylcyclooctene lignan class, which encompasses schineolignin A, gomisin L_2, schisandrin, schisandrin A, schisandrin B, schisandrin C, schisanhenol, schisanchinin C, and schisandrol B. Notably, several of these lignans (schisandrin C, schisandrin A, schisandrin B, schisandrin, and schisandrol B) have been confirmed through comparison with standard samples and are relatively abundant in SCF.

In contrast, only schisandrin C was identified in SSF through comparison with standard samples and found to cross the BBB. The total lignin extracts of SCF have been demonstrated to possess robust anti-neuroinflammatory effects.[37] In addition, several studies have reported that schisandrin A, schisandrin B, schisandrin C, schisandrin, and schisandrol B – compounds isolated from SCF – can alleviate neuroinflammation *in vitro* and *in vivo* models, supporting their potential roles in the treatment of VCI.[19,38-41] Taken together, these findings suggest that the primary pharmacological effects of SCF likely stem from the specific compounds mentioned above.

5. Conclusion

The present study demonstrates that both SCF and SSF can effectively ameliorate VCI, at least in part, by enhancing anti-neuroinflammatory and antioxidative stress responses. However, SCF exhibits superior effects in improving cognitive impairment compared to SSF, likely due to its higher structural diversity of biphenylcyclooctene-type lignans. This study provides scientifically valuable data on the therapeutic differences between SCF and SSF in the treatment of VCI and offers insights relevant to clinical applications.

Acknowledgments

None.

Funding

This work was supported by the CAMS Innovation Fund for Medical Sciences (2023-I2M-QJ-013, 2021-I2M-1-031, 2023-I2M-2-006, and 2022-I2M-2-002), the Beijing Natural Science Foundation (No. Z220019), and National Natural Science Foundation of China (No. U23A20511, No. 82304708).

Conflict of interest

The authors declare that they have no known competing financial interests or personal relationships that could have appeared to influence the work reported in this paper.

Author contributions

Conceptualization: Pei Ma
Data curation: Yucen Zou, Bin Li, Meiqi Wang, Jianuo Zhang, Qi Xiao, Chunyan Yang
Formal analysis: Yucen Zou, Bin Li, Meiqi Wang, Xiaomeng Xie, Jianuo Zhang, Qi Xiao, Jiushi Liu
Investigation: Jiushi Liu
Methodology: Haitao Sun, Bengang Zhang
Writing – original draft: Yucen Zou, Bin Li, Pei Ma
Writing – review & editing: Haitao Liu

Ethics approval and consent to participate

BV2 cells were purchased from the Chinese Academy of Medical Sciences (Beijing, China). All animal experimental procedures in this study followed the Guide for the Care and Use of Laboratory Animals (National Institutes of Health), approved by the Experimental Animal Ethical Committee of the Institute of Medicinal Plant Development, Chinese Academy of Medical Sciences (SLXD-20230425013).

Consent for publication

Not applicable.

Availability of data

The data that support the findings of this study are available from the corresponding author upon reasonable request.

References

1. Wang Z, Han B, Qi J, Cao X, Gu H, Sun J. Chuanzhitongluo capsule improves cognitive impairment in mice with chronic cerebral poperfusion via the cholinergic anti-inflammatory pathway. *Exp Gerontol*. 2024;189:112407.

   doi: 10.1016/j.exger.2024.112407

2. Lou T, Wu H, Feng M, *et al*. Integration of metabolomics and transcriptomics reveals that da chuanxiong formula improves vascular cognitive impairment via Acsl4/Gpx4 mediated ferroptosis. *J Ethnopharmacol*. 2024;325:117868.

   doi: 10.1016/j.jep.2024.117868

3. Hao S, He Q, Yuan Y, Mu Q. The protective effects of Irbesartan in cognitive impairment in hypertension. *Aging* (*Albany NY*). 2024;16(6):5065-5076.

   doi: 10.18632/aging.205589

4. Li S, Xiao Z. Recent research progress on the use of transcranial magnetic stimulation in the treatment of vascular cognitive impairment. *Neuropsychiatr Dis Treat*. 2024;20:1235-1246.

   doi: 10.2147/ndt.S467357

5. Lu H, Zhang J, Liang Y, *et al*. Network topology and machine learning analyses reveal microstructural white matter changes underlying Chinese medicine Dengzhan Shengmai treatment on patients with vascular cognitive impairment. *Pharmacol Res*. 2020;156:104773.

   doi: 10.1016/j.phrs.2020.104773

6. Lv S, Wang Q, Zhang X, *et al*. Mechanisms of Multi-Omics and network pharmacology to explain traditional Chinese medicine for vascular cognitive impairment: A narrative review. *Phytomedicine*. 2024;123:155231.

   doi: 10.1016/j.phymed.2023.155231

7. Hu WH, Mak SH, Zheng ZY, *et al*. Shexiang Baoxin Pill, a traditional chinese herbal formula, rescues the cognitive

impairments in APP/PS1 transgenic mice. *Front Pharmacol*. 2020;11:1045.

doi: 10.3389/fphar.2020.01045

8. Sowndhararajan K, Deepa P, Kim M, Park SJ, Kim S. An overview of neuroprotective and cognitive enhancement properties of Lignans from *Schisandra chinensis*. *Biomed Pharmacother.* 2018;97:958-968.

doi: 10.1016/j.biopha.2017.10.145

9. Zhang M, Xu L, Yang H. *Schisandra chinensis* fructus and its active ingredients as promising resources for the treatment of neurological diseases. *Int J Mol Sci*. 2018;19(7):1970.

doi: 10.3390/ijms19071970

10. Rybnikár M, Malaník M, Smejkal K, *et al*. Dibenzocyclooctadiene Lignans from *Schisandra chinensis* with anti-inflammatory effects. *Int J Mol Sci*. 2024;25(6):3465.

doi: 10.3390/ijms25063465

11. Li B, Xiao Q, Zhang JN, *et al*. Exploring the active compounds and potential mechanism of the anti-nonalcoholic fatty liver disease activity of the fraction from *Schisandra chinensis* fruit extract based on multi-technology integrated network pharmacology. *J Ethnopharmacol*. 2023;301:115769.

doi: 10.1016/j.jep.2022.115769

12. Huang S, Zhang D, Li Y, *et al*. *Schisandra sphenanthera*: A comprehensive review of its botany, phytochemistry, pharmacology, and clinical applications. *Am J Chin Med*. 2021;49(7):1577-1622.

doi: 10.1142/s0192415x21500749

13. Yang K, Qiu J, Huang Z, *et al*. A comprehensive review of ethnopharmacology, phytochemistry, pharmacology, and pharmacokinetics of *Schisandra chinensis* (Turcz.) Baill. And *Schisandra sphenanthera* Rehd. et Wils. *J Ethnopharmacol*. 2022;284:114759.

doi: 10.1016/j.jep.2021.114759

14. Jafernik K, Motyka S, Calina D, Sharifi-Rad J, Szopa A. Comprehensive review of dibenzocyclooctadiene lignans from the *schisandra* genus: Anticancer potential, mechanistic insights and future prospects in oncology. *Chin Med*. 2024;19(1):17.

doi: 10.1186/s13020-024-00879-0

15. Liu SQ, Yang YP, Hussain N, *et al*. Dibenzocyclooctadiene Lignans from the Family *Schisandraceae*: A review of phytochemistry, structure-activity relationship, and hepatoprotective effects. *Pharmacol Res*. 2023;195:106872.

doi: 10.1016/j.phrs.2023.106872

16. Kim DH, Hung TM, Bae KH, *et al*. Gomisin a improves scopolamine-induced memory impairment in mice. *Eur J Pharmacol*. 2006;542(1):129-135.

doi: 10.1016/j.ejphar.2006.06.015

17. Li XL, Zhao X, Xu X, *et al*. Schisantherin a recovers Aβ-induced neurodegeneration with cognitive decline in mice. *Physiol Behav*. 2014;132:10-16.

doi: 10.1016/j.physbeh.2014.04.046

18. Xu MJ, Yan TX, Fan KY, *et al*. Polysaccharide of *Schisandra chinensis* fructus ameliorates cognitive decline in a mouse model of Alzheimer's disease. *J Ethnopharmacolo.* 2019;237:354-365.

doi: 10.1016/j.jep.2019.02.046

19. Hu D, Cao Y, He R, *et al*. Schizandrin, an antioxidant Lignan from *Schisandra chinensis*, ameliorates Aβ1-42-induced memory impairment in mice. *Oxid Med Cell Longev*. 2012;2012:721721.

doi: 10.1155/2012/721721

20. Zhao X, Liu CM, Xu MJ, Li XL, Bi KS, Jia Y. Total Lignans of *Schisandra chinensis* Ameliorates Aβ(1-42)-induced neurodegeneration with cognitive impairment in mice and primary mouse neuronal cells. *PLoS One*. 2016;11(4):e0152772.

doi: 10.1371/journal.pone.0152772

21. Shibata M, Ohtani R, Ihara M, Tomimoto H. White matter lesions and glial activation in a novel mouse model of chronic cerebral hypoperfusion. *Stroke*. 2004;35(11):2598-2603.

doi: 10.1161/01.Str.0000143725.19053.60

22. Zhang YL, Chopp M, Meng YL, *et al*. Effect of exosomes derived from multipluripotent mesenchyrnal stromal cells on functional recovery and neurovascular plasticity in rats after traumatic brain injury. *J Neurosurg*. 2015;122(4):856-867.

doi: 10.3171/2014.11.Jns14770

23. Wan YS, You Y, Ding QY, *et al*. Triptolide protects against white matter injury induced by chronic cerebral hypoperfusion in mice. *Acta Pharmacol Sin*. 2022;43(1):15-25.

doi: 10.1038/s41401-021-00637-0

24. Chen S, Li Q, Shi H, Li F, Duan Y, Guo, Q. New insights into the role of mitochondrial dynamics in oxidative stress-induced diseases. *Biomed Pharmacother*. 2024;178:117084.

doi: 10.1016/j.biopha.2024.117084

25. Ma P, Zhang R, Xu L, Liu H, Xiao P. The neuroprotective effects of coreopsis tinctoria and its mechanism: interpretation of network pharmacological and experimental data. *Front Pharmacol*. 2021;12:791288.

doi: 10.3389/fphar.2021.791288

26. Mendie LE, Hemalatha S. Bioactive compounds from nyctanthes arbor tristis linn as potential inhibitors of Janus Kinases (Jaks) involved in rheumatoid arthritis. *Appl Biochem Biotechnol*. 2023;195(1):314-330.

doi: 10.1007/s12010-022-04121-1

27. Yao JY, Yang YL, Chen WJ, Fan HY. Exploring the therapeutic potential of Qi Teng Mai Ning recipe in ischemic stroke and

vascular cognitive impairment. *Trad Med Res*. 2024;9:57.

28. Fu Z, Wang X, Fan Y, *et al*. Brozopine ameliorates cognitive impairment via upregulating Nrf2, antioxidation and anti-inflammation activities. *Front Pharmacol*. 2024;15:1428455.

    doi: 10.3389/fphar.2024.1428455

29. Cai H, Cai T, Zheng H, *et al*. The neuroprotective effects of danggui-shaoyao san on vascular cognitive impairment: Involvement of the role of the low-density lipoprotein receptor-related protein. *Rejuvenation Res*. 2020;23:420-433.

    doi: 10.1089/rej.2019.2182

30. Zheng V, Wong G. Neuroinflammation responses after subarachnoid hemorrhage: A review. *J Clin Neurosci*. 2017;42:7-11

    doi: 10.1016/j.jocn.2017.02.001

31. Kim T, Vemuganti R. Mechanisms of Parkinson's disease-related proteins in mediating secondary brain damage after cerebral ischemia. *J Cereb Blood Flow Metab*. 2017;37(6):1910-1926.

    doi: 10.1177/0271678x17694186

32. Ziemka-Nalecz M, Jaworska J, Zalewska T. Insights into the neuroinflammatory responses after neonatal hypoxia-ischemia. *J Neuropathol Exp Neurol*. 2017;76(8):644-654.

    doi: 10.1093/jnen/nlx046

33. Xiao ZH, Xiao W, Li GL. Research progress on the pharmacological action of Schisantherin A. *Evid Based Complement Alternat Med*. 2022;2022:6420865.

    doi: 10.1155/2022/6420865

34. Jung CH, Hong MH, Kim JH, *et al*. Protective effect of a Phenolie-rich fraction from *Schisandra chinensis* against H_2O_2-induced apoptosis in SH-SY5Y cells. *J Pharmacy Pharmacol*. 2007;59(3):455-462.

    doi: 10.1211/jpp.59.3.0016

35. Khan MB, Hoda MN, Vaibhav K, *et al*. Remote ischemic postconditioning: Harnessing endogenous protection in a murine model of vascular cognitive impairment. *Transl Stroke Res*. 2015;6(1):69-77.

    doi: 10.1007/s12975-014-0374-6

36. Hattori Y, Enmi JI, Iguchi S, *et al*. Substantial reduction of parenchymal cerebral blood flow in mice with bilateral common carotid artery stenosis. *Sci Rep*. 2016;6(1):32179.

    doi: 10.1038/srep32179

37. Wang JY, Zhang GL, Yang YF, *et al*. *Schisandra chinensis* Lignans exert antidepressant effects by promoting BV2 microglia polarization toward the M2 phenotype through the activation of the cannabinoid receptor type-2-signal transducer and activator of transcription 6 pathway. *J Agric Food Chem*. 2022;70(44):14157-14169.

    doi: 10.1021/acs.jafc.2c04565

38. Song FJ, Zeng KW, Liao LX, Yu Q, Tu PF, Wang XM. Schizandrin A inhibits microglia-mediated neuroninflammation through inhibiting TRAF6-NF-κB and JAK2-STAT3 signaling pathways. *PLoS One*. 2016;11(2):e0149991.

    doi: 10.1371/journal.pone.0149991

39. Zeng KW, Zhang T, Fu H, Liu GX, Wang XM. Schisandrin B exerts anti-neuroinflammatory activity by inhibiting the toll-like receptor 4-dependent MyD88/IKK/NF-κB signaling pathway in lipopolysaccharide-induced microglia. *Eur J Pharmacol*. 2012;692(1-3):29-37.

    doi: 10.1016/j.ejphar.2012.05.030

40. Chen S, Ding YH, Shi SS, Tu XK. Schisandrin B inhibits NLRP3 inflammasome pathway and attenuates early brain injury in rats of subarachnoid hemorrhage. *Chin J Integr Med*. 2022;28(7):594-602.

    doi: 10.1007/s11655-021-3348-z

41. Qun E, Tang M, Zhang X, *et al*. Protection of seven dibenzocyclooctadiene lignans from *schisandra chinensis* against serum and glucose deprivation injury in SH-SY5Y cells. *Cell Biol Int*. 2015;39(12):1418-1424.

    doi: 10.1002/cbin.10537